







Cite this: *Dalton Trans.*, 2023, **52**, 2219Received 19th November 2022,
Accepted 8th February 2023

DOI: 10.1039/d2dt03731a

rsc.li/dalton

A “gold standard” computational proof for the existence of gold(III) aurophilicity†

Daniel Blasco, ^{*,†a,b} Félix Reboiro, ^{†a} Dage Sundholm, ^b M. Elena Olmos, ^a Miguel Monge ^{*,†a} and José M. López-de-Luzuriaga ^{*,†a}

The existence of aurophilic gold(III)–gold(III) interactions has for a long time been neglected due to structural arguments and comparison with the aurophilicity of gold(I) compounds. We show with calculations at the CCSD(T) level of theory that the $[\text{Au}^{\text{III}}(\text{CH}_3)_3(\text{NH}_3)]_2$ dimer has a metallophilic dispersion interaction between the gold(III) atoms of 10.5 kJ mol^{-1} . The aurophilic interaction is illustrated by topological QTAIM calculations and IRI analysis.

The concept of *metallophilicity* encompasses attractive van der Waals interactions between pairs, strings, or clusters of closed- (d^{10}, s^2d^{10}) or seemingly closed-shell (d^8) late transition metals that originate from the relativistic mass increase of the s electrons. Among metallophilic interactions, *aurophilicity* has a privileged status due to its noticeable strength of $30\text{--}50 \text{ kJ mol}^{-1}$ that affects the crystalline structure and bulk properties of gold(I)-containing materials.^{1–3} The character of the interaction is supported by ever-growing irrefutable structural evidence and by computational simulation at post-Hartree–Fock (HF) and density functional theory (DFT) levels that consider van der Waals interactions.⁴ A gold–gold distance of less than twice its van der Waals radius is considered aurophilic. The radius proposed by Bondi for gold, 1.62 \AA , is usually chosen,⁵ although longer values have been reported, such as Allinger’s 2.43 \AA .^{6,7}

Whereas the existence of the aurophilicity between gold(I) atoms ($\text{Au}^{\text{I}}\cdots\text{Au}^{\text{I}}$; $[\text{Au}^{\text{I}}]: [\text{Xe}] 4f^{14}5d^{10}$) is now out of debate, there is still room for doubts regarding the presence of analo-

gous aurophilicity between gold(III) atoms ($\text{Au}^{\text{III}}\cdots\text{Au}^{\text{III}}$; $[\text{Au}^{\text{III}}]: [\text{Xe}] 4f^{14}5d^8$). There is still no consensus in the scientific community on its existence.⁸ Two factors are thought to prevent the formation of $\text{Au}^{\text{III}}\cdots\text{Au}^{\text{III}}$ interactions: (i) the depletion of electron density, since gold(III) is a hard Pearson acid, whereas gold(I) is a soft one, and (ii) the relativistic effects of gold(III) are less pronounced as compared to gold(I).⁹

However, this reasoning is only enough for explaining the weaker interaction between $\text{Au}^{\text{III}}\cdots\text{Au}^{\text{III}}$ as compared to the $\text{Au}^{\text{I}}\cdots\text{Au}^{\text{I}}$ one but not to rule out its existence. In our opinion, the different orbital structure (d^8 vs. d^{10}) and coordination environment (square planar vs. linear) of gold(III) may not prevent the *existence* of dispersive forces like aurophilicity. Moreover, the contribution of relativistic effects to the aurophilic attraction is not fundamental, accounting for only 22–27% of the total interaction energy.^{10,11} There are some experimental and computational results that support our claim that $\text{Au}^{\text{III}}\cdots\text{Au}^{\text{III}}$ interactions contribute to the stabilization of gold(III) dimers and polymers, even though they are weaker and overruled by other secondary interactions. The following studies suggest that there is a weak van der Waals-type interaction between the gold(III) atoms:

(i) Mendizabal and Pyykkö calculated at the second order Møller–Plesset (MP2) level of theory a stabilizing interaction of -34.94 or $-56.75 \text{ kJ mol}^{-1}$ between the two molecules of the $[\text{Au}^{\text{III}}\text{Cl}_3(\text{PH}_3)]_2$ dimer when the dipole moments of the monomers were perpendicular or antiparallel, respectively. There was an attraction of $-20.71 \text{ kJ mol}^{-1}$ even at the HF level, when the molecules were oriented in a perpendicular fashion.¹²

(ii) In 2005, Klapötke *et al.* prepared a series of ammonium tetraazidoaurate(III) ($[\text{Q}[\text{Au}^{\text{III}}(\text{N}_3)_4]]$; $\text{Q} = \text{NMe}_4, \text{NMe}_2\text{H}_2, \text{NH}_4$) complexes. The crystal structure of $(\text{NMe}_4)[\text{Au}^{\text{III}}(\text{N}_3)_4]$ has one-dimensional chains of anions linked by $\text{Au}^{\text{III}}\cdots\text{Au}^{\text{III}}$ contacts, whose bond distances are $3.507(3), 3.584(3) \text{ \AA}$.¹³ However, an attractive nature of such contacts was not obtained in molecular structure optimizations of a $[\text{Au}^{\text{III}}(\text{N}_3)_4]^{2-}$ dimer at the DFT level using the B3LYP functional. The dimer dissociated.

^aDepartamento de Química, Centro de Investigación en Síntesis Química (CISQ), Universidad de La Rioja, Madre de Dios 53, 26006 Logroño, Spain. E-mail: miguel.monge@unirioja.es, josemaria.lopez@unirioja.es

^bDepartment of Chemistry, Faculty of Science, University of Helsinki, P.O. Box 55 (A. I. Virtasen aukio 1), FIN-00014 Helsinki, Finland. E-mail: daniel.blasco@helsinki.fi

†Electronic supplementary information (ESI) available: Computational details, interaction energy calculations on molecules 1–3, EDA of molecule 1, IRI analysis of molecule 2, Cartesian coordinates of molecules 1–3, $[\text{Au}^{\text{III}}(\text{CH}_3)_3(\text{NH}_3)]\cdots[(\text{CH}_4)_3(\text{NH}_3)]$ and $[(\text{CH}_4)_3(\text{NH}_3)]_2$. See DOI: <https://doi.org/10.1039/d2dt03731a>

‡These authors contributed equally.

(iii) A year later, Doerrer *et al.* synthesized up to eleven double salts of $[\text{Pt}^{\text{II}}(\text{tpy})\text{X}]^+$ and $[\text{Au}^{\text{III}}(\text{bpy})\text{X}_2]^+$ ($\text{tpy} = 2,2':6',2''$ -terpyridine; $\text{bpy} = 2,2'$ -bipyridine; $\text{X} = \text{Cl}, \text{Br}, \text{CN}$) cations that were prepared by anion metathesis in aqueous solution.¹⁴ Among them, the crystal structures of $[\text{Au}^{\text{III}}(\text{bpy})\text{Cl}_2][\text{Au}^{\text{III}}\text{Br}_4]$ and $[\text{Au}^{\text{III}}(\text{bpy})\text{Br}_2][\text{Au}^{\text{III}}\text{Br}_4]$ with the gold(III)-gold(III) ion pairs are noteworthy, since they have $\text{Au}^{\text{III}}(\text{cation})\cdots\text{Au}^{\text{III}}(\text{anion})$ distances of 3.518(1) Å and *ca.* 3.54 Å, respectively. The quality of $[\text{Au}^{\text{III}}(\text{bpy})\text{Br}_2][\text{Au}^{\text{III}}\text{Br}_4]$ was unpubliable. A similar study was reported in 2015 by Haukka *et al.* including quantum theory of atoms in molecules (QTAIM) calculations of the topology of the charge density.⁷ The authors proposed a combination of structural measurements and bond critical point (BCP) descriptors to identify $\text{Au}^{\text{III}}\cdots\text{Au}^{\text{III}}$ aurophilicity. They also report $\text{Au}^{\text{III}}\cdots\text{Au}^{\text{III}}$ interaction energies at the DFT/PBE0 level of theory in the range 3.6–9.3 kJ mol^{−1}.

(iv) Extremely short intramolecular $\text{Au}^{\text{III}}\cdots\text{Au}^{\text{III}}$ distances ranging between 2.984–3.080 Å were obtained by Bessonov *et al.* for the molecular structure of doubly supported dimethylgold(III) carboxylates $[\{\text{Au}^{\text{III}}(\text{CH}_3)_2\}_2(\mu\text{-OC}(\text{R})\text{O})_2]$; $\text{R} = \text{H}, \text{CF}_3, \text{C}(\text{CH}_3)_3, \text{Ph}$.¹⁵

(v) Che *et al.* contributed to the search for these interactions with the article from 2012 where they prepared $[\text{Au}^{\text{III}}(\text{C}^{\wedge}\text{N}^{\wedge}\text{N})(\text{C}\equiv\text{CC}_6\text{H}_4\text{-4-NMe}_2)](\text{PF}_6)$ ($\text{C}^{\wedge}\text{N}^{\wedge}\text{N} = 6\text{-phenyl-2,2'-bipyridine}$) with the shortest unsupported $\text{Au}^{\text{III}}\cdots\text{Au}^{\text{III}}$ distance to date of 3.495 Å.¹⁶

The gold(III) ions of examples (ii) and (v) would not be expected to aggregate by $\text{Au}^{\text{III}}\cdots\text{Au}^{\text{III}}$ contacts based on Coulomb repulsion, and therefore gold(III) aurophilicity is reasonably invoked in these cases. Also note that in examples (iii) and (iv) the presumed gold(III) aurophilic interaction is assisted by Coulomb attraction and ligand support, respectively.

Here, we demonstrate that at the “gold standard” level of theory *i.e.*, at the coupled cluster singles and doubles level with a perturbative treatment of the triples (CCSD(T)) in combination with the def2-TZVP basis sets,¹⁷ the $\text{Au}^{\text{III}}\cdots\text{Au}^{\text{III}}$ interactions explain a part of the total interaction energy between neutral gold(III) complexes.

For achieving a clearer-as-possible description of the $\text{Au}^{\text{III}}\cdots\text{Au}^{\text{III}}$ interaction without losing chemical representativeness, we have built a very simple dimer model by substituting the C_3N donor atoms of the well-known bis-orthometallated $[\text{Au}^{\text{III}}(\text{C}^{\wedge}\text{N}^{\wedge}\text{C})(\text{alkynyl})]$ complexes¹⁸ with methyl and ammonia ligands, respectively. The small size of $[\text{Au}^{\text{III}}(\text{CH}_3)_3(\text{NH}_3)_2]$ (Fig. 1, inset; molecule 1) allows us to employ correlated *ab initio* levels of theory such as RI-MP2/def2-TZVP and CCSD(T)/def2-TZVP. The computational details are given in the ESI.† The molecular structure of 1 optimized at the RI-MP2/def2-TZVP level has been employed in the calculations of the interaction energies. The potential energy curves (PECs) have been obtained by stretching the $\text{Au}^{\text{III}}\cdots\text{Au}^{\text{III}}$ distance to the selected values, without reoptimization of the rest of the dimer. The counterpoise-corrected RHF, RI-MP2 and CCSD(T) interaction energies (ΔE_{int} , eqn (S1)†) as functions of the $\text{Au}^{\text{III}}\cdots\text{Au}^{\text{III}}$ distance (R) are plotted in Fig. 1. The equilibrium distances (R_e)

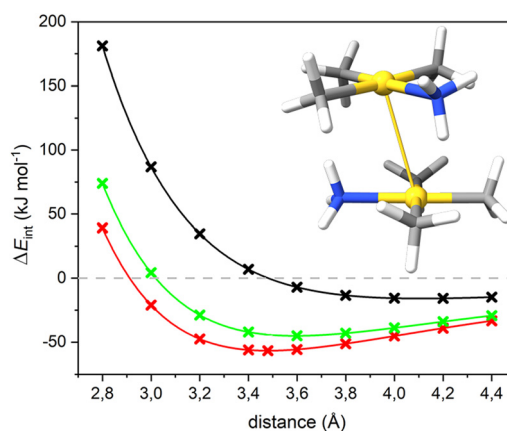


Fig. 1 The total interaction energy as a function of the $\text{Au}^{\text{III}}\cdots\text{Au}^{\text{III}}$ distance for molecule 1, calculated at the RHF (black), RI-MP2 (red) and CCSD(T) (green) levels of theory. Inset: RI-MP2/def2-TZVP optimized structure of molecule 1; colour code: C, grey; H, white; Au, yellow; N, blue.

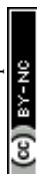
and interaction energies ($\Delta E_{\text{int}}(R_e)$) derived from fitting the points to the Herschbach–Laurie four-parameter function (eqn (S2)†) are given in Table 1.

The PECs are markedly different depending on the chosen level of theory. In other words, the PEC depends on how electron correlation is considered in the computational framework. At the RHF level that does not consider electron correlation, the interaction curve is non-bonding and flat at long distances, although an overall binding of the dimer ($\Delta E_{\text{int}} < 0$) is found at distances longer than *ca.* 3.48 Å. This finding agrees with the results obtained by Mendizabal and Pyykkö for antiparallel $[\text{Au}^{\text{III}}\text{Cl}_3(\text{PH}_3)]_2$, and the same explanation based on long-range dipole–dipole attraction may be invoked here. When electron correlation is considered an interaction minimum is predicted, suggesting a dispersive origin for the intermolecular attraction. Whereas both RI-MP2 and CCSD(T) predict a minimum, RI-MP2 calculations find it at a shorter distance of 3.48 Å as compared to 3.59 Å at the CCSD(T) level. The binding energy of 56.64 kJ mol^{−1} obtained at the RI-MP2 level is also somewhat larger than the one of 45.05 kJ mol^{−1} calculated at CCSD(T) level, which is in line with the notion that MP2 overestimates van der Waals interaction energies. The total interaction energy between the monomers of 1 can

Table 1 Gold(III)⋯Gold(III) Equilibrium Distances (R_e in Å) and Interaction Energies (ΔE_{int} in kJ mol^{−1}) of Molecule 1 at the RHF, RI-MP2 and CCSD(T) levels of theory^a

Level of theory	R_e	$-\Delta E_{\text{int}}(R_e)$			
		Total	$\text{Au}^{\text{III}}\cdots[\text{ligand}]$	$[\text{ligand}]\cdots[\text{ligand}]$	$\text{Au}^{\text{III}}\cdots\text{Au}^{\text{III}}$
RHF	4.11	15.9	—	—	—
RI-MP2	3.48	56.6	25.3	10.7	16.7
CCSD(T)	3.59	45.1	23.1	11.6	10.5

^a $-\Delta E_{\text{int}}(\text{Au}^{\text{III}}\cdots\text{Au}^{\text{III}}) = \Delta E_{\text{int}}(\text{total}) - 2 \times \Delta E_{\text{int}}(\text{Au}^{\text{III}}\cdots[\text{ligand}]) + \Delta E_{\text{int}}([\text{ligand}]\cdots[\text{ligand}])$.



be approximated to the sum of $\text{Au}^{\text{III}}\cdots\text{Au}^{\text{III}}$, twice $\text{Au}^{\text{III}}\cdots[\text{ligand}]$, and $[\text{ligand}]\cdots[\text{ligand}]$ contributions $\{[\text{ligand}] = [(\text{CH}_3)_3(\text{NH}_3)]\}$. The contribution from the $\text{Au}^{\text{III}}\cdots[\text{ligand}]$ interactions to the total interaction energy has been partially removed by subtracting twice that calculated for a monomer of **1** and the saturated ligands of the other monomer at the RI-MP2 and CCSD(T) $\text{Au}^{\text{III}}\cdots\text{Au}^{\text{III}}$ equilibrium distances, respectively. The extra $[\text{ligand}]\cdots[\text{ligand}]$ interaction energy removed in this way has been restored by adding that of the saturated ligands of $[(\text{CH}_4)_3(\text{NH}_3)]_2$ (see Fig. S1 and the ESI for further details†). Correcting for $\text{Au}^{\text{III}}\cdots[\text{ligand}]$ and $[\text{ligand}]\cdots[\text{ligand}]$ interaction leads to an approximate attractive interaction energy of 16.7 (RI-MP2) and 10.5 kJ mol^{-1} (CCSD(T)) when considering only the $\text{Au}^{\text{III}}\cdots\text{Au}^{\text{III}}$ interactions.

We have repeated this procedure with Klapötke's anionic $[\text{Au}^{\text{III}}(\text{N}_3)_4]_2^{2-}$ dimer (molecule **2**)¹³ and with a theoretical cationic $\{cis\text{-}[\text{Au}^{\text{III}}(\text{CH}_3)_2(\text{NH}_3)_2]\}_2^{2+}$ dimer (molecule **3**) as a model of the interaction found in $[\text{Au}^{\text{III}}(\text{C}^{\wedge}\text{N}^{\wedge}\text{N})(\text{C}\equiv\text{CC}_6\text{H}_4\text{-4-NMe}_2)](\text{PF}_6)$,¹⁶ as proofs of concept. Due to the larger size of **2** and the repulsive character of the interaction found within **3** (*vide infra*), we only report results obtained at the RHF/def2-TZVP and RI-MP2/def2-TZVP levels of theory. We also found that optimizing the bound dimer of **2** at the RI-DFT/B3LYP-D3(BJ)/def2-TZVP level of theory results in its dissociation. However, if the same calculation is done at the RI-MP2/def2-TZVP level, a short $\text{Au}^{\text{III}}\cdots\text{Au}^{\text{III}}$ distance of 3.09 Å is obtained (Fig. S2,† inset). The PECs of **2** are repulsive at all distances due to the coulombic force between the anions, but an MP2 minimum at *ca.* 3.21 Å is found (Fig. S2†). Thus, $\text{Au}^{\text{III}}\cdots\text{Au}^{\text{III}}$ interactions may play a role in directing the crystal packing of $[\text{NMe}_4][\text{Au}^{\text{III}}(\text{N}_3)_4]$. However, the free optimization of **3** at the same level of theory as **2** led to the complete dissociation of the dimer. A starting structure was therefore obtained by fixing the $\text{Au}^{\text{III}}\cdots\text{Au}^{\text{III}}$ distance during the optimization. The absence of a minimum in the PECs of **3** (Fig. S3†) shows that cation-cation repulsion overcomes gold(III) auriphilicity if no other interligand interactions are present.

The RI-DFT/PBE0-D3(BJ)/def2-TZVP interaction energy (ΔE_{int})§§ between the gold(III) monomers of molecule **1** has been decomposed into:

$$\Delta E_{\text{int}} = \Delta E_{\text{ele}} + \Delta E_{\text{ex-rep}} + \Delta E_{\text{orb}} + \Delta E_{\text{corr}} + \Delta E_{\text{disp}}$$

where ΔE_{ele} is the quasiclassical electrostatic interaction, $\Delta E_{\text{ex-rep}}$ is the Pauli exchange repulsion, ΔE_{orb} is the orbital relaxation, ΔE_{corr} is the correlation interaction, and ΔE_{disp} is the additional van der Waals interaction energy obtained with the D3(BJ) correction. The relative contribution of each attractive energy contribution to the total interaction energy, except the repulsive $\Delta E_{\text{ex-rep}}$, is plotted in Fig. 2 as a function of the $\text{Au}^{\text{III}}\cdots\text{Au}^{\text{III}}$ distance. For a plot of the absolute values see Fig. S4.† Note that, at the $\text{Au}^{\text{III}}\cdots\text{Au}^{\text{III}}$ equilibrium distance of 3.40–3.60 Å, the correlation contribution has its maximum and surpasses that for orbital relaxation. Thus, the inter-dimer attraction arises from dispersion interaction and from electrostatic interaction as obtained at the RHF level.

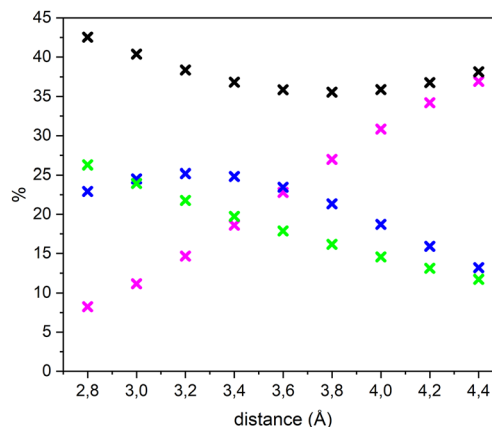


Fig. 2 Relative contribution of ΔE_{ele} (black), ΔE_{orb} (green), ΔE_{corr} (blue) and ΔE_{disp} (pink) to the stabilization of molecule **1**.

The CCSD(T) electron density of molecule **1** has been examined using QTAIM¹⁹ and topological calculations with the interaction region indicator (IRI) analysis method.²⁰ The relationship between the QTAIM (3, −1) BCPs, bond paths *i.e.*, the maximal gradient path connecting two BCPs, and $\text{sign}(\lambda_2) \times \rho_e$ -weighted IRI isosurfaces in a single image is a powerful tool for gaining visual insight into the covalent and non-covalent interactions. Fig. 3 shows how molecule **1** is bound by attractive, van der Waals, and repulsive interactions and their strength. A BCP is found in the bond path connecting the two gold(III) atoms with an electron density ($\rho_e(\text{BCP})$) of 0.0055 e Å^3 . Its Laplacian ($\nabla^2[\rho_e(\text{BCP})]$) is 0.0136. The $\rho_e(\text{BCP})$

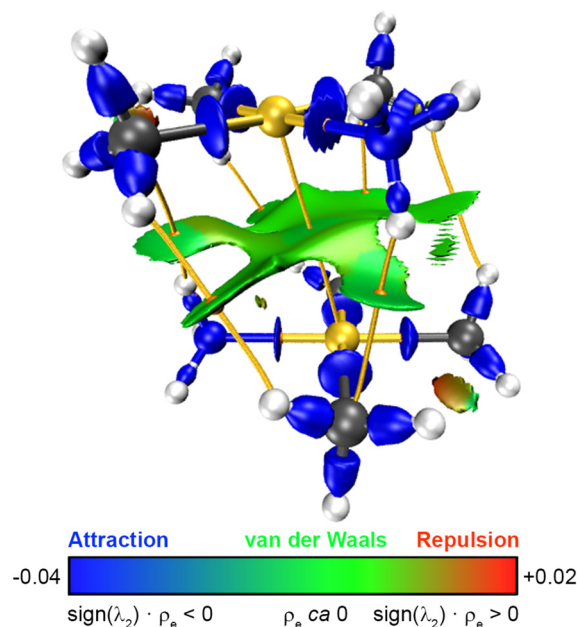


Fig. 3 The QTAIM (3, −1) BCPs (orange dots), bond paths (yellow strings) and the IRI isosurface (isovalue = 1.0) are superimposed for molecule **1**. The RGB colour scale refers to the IRI isosurface (adapted from ref. 16). Colour code: C, grey; H, white; Au, yellow; N, blue.

JML, MM and MEO designed the project. DS and MM provided the computational resources. DB and FR conducted the calculations. All authors have contributed to the text of the final version of the manuscript. DB and FR contributed equally.

§The energy decomposition analysis (EDA) is currently implemented in TURBOMOLE v.7.5.1 at the RHF and DFT levels of theory only.

- 1 N. Mirzadeh, S. H. Privér, A. J. Blake, H. Schmidbaur and S. K. Bhargava, *Chem. Rev.*, 2020, **120**, 7551–7591.
- 2 H. Schmidbaur and A. Schier, *Chem. Soc. Rev.*, 2012, **41**, 370–412.
- 3 H. Schmidbaur and A. Schier, *Chem. Soc. Rev.*, 2008, **37**, 1931–1951.
- 4 P. Pyykkö, *Angew. Chem., Int. Ed.*, 2004, **43**, 4412–4456.
- 5 A. Bondi, *J. Phys. Chem.*, 1964, **68**, 441–451.
- 6 N. L. Allinger, X. Zhou and J. Bergsma, *J. Mol. Struct.: THEOCHEM*, 1994, **312**, 69–83.
- 7 A. N. Chernyshev, M. V. Chernysheva, P. Hirva, V. Y. Kukushkin and M. Haukka, *Dalton Trans.*, 2015, **44**, 14523–14531.
- 8 L. Rocchigiani and M. Bochmann, *Chem. Rev.*, 2021, **121**, 8364–8451.
- 9 P. Schwerdtfeger, P. D. W. Boyd, S. Brienne and A. K. Burrell, *Inorg. Chem.*, 1992, **31**, 3411–3422.
- 10 P. Pyykko, N. Runeberg and F. Mendizabal, *Chem. – Eur. J.*, 1997, **3**, 1451–1457.
- 11 N. Runeberg, M. Schütz and H.-J. Werner, *J. Chem. Phys.*, 1999, **110**, 7210–7215.
- 12 F. Mendizabal and P. Pyykkö, *Phys. Chem. Chem. Phys.*, 2004, **6**, 900–905.
- 13 T. M. Klapötke, B. Krumm, J.-C. Galvez-Ruiz and H. Nöth, *Inorg. Chem.*, 2005, **44**, 9625–9627.
- 14 R. Hayoun, D. K. Zhong, A. L. Rheingold and L. H. Doerrer, *Inorg. Chem.*, 2006, **45**, 6120–6122.
- 15 A. A. Bessonov, N. B. Morozova, N. V. Kurat'eva, I. A. Baidina, N. V. Gel'fond and I. K. Igumenov, *Russ. J. Coord. Chem.*, 2008, **34**, 73–80.
- 16 W. Lu, K. T. Chan, S.-X. Wu, Y. Chen and C.-M. Che, *Chem. Sci.*, 2012, **3**, 752–755.
- 17 J. Řezáč and P. Hobza, *J. Chem. Theory Comput.*, 2013, **9**, 2151–2155.
- 18 C. Bronner and O. S. Wenger, *Dalton Trans.*, 2011, **40**, 12409–12420.
- 19 R. F. W. Bader, *Chem. Rev.*, 1991, **91**, 893–928.
- 20 T. Lu and Q. Chen, *Chem.: Methods*, 2021, **1**, 231–239.
- 21 R. Bianchi, G. Gervasio and D. Marabello, *Inorg. Chem.*, 2000, **39**, 2360–2366.
- 22 R. F. W. Bader, *J. Phys. Chem. A*, 2009, **113**, 10391–10396.
- 23 R. F. W. Bader, *J. Phys. Chem. A*, 1998, **102**, 7314–7323.

There are no conflicts to declare.

The research has been supported by MCIN/AEI/10.13039/501100011033 through project PID2019-104379RB-C22, and by The Academy of Finland through project 340583. DB acknowledges Universidad de La Rioja for the concession of a Margarita Salas post-doctoral scholarship financed by the Spanish Ministerio de Universidades and the European Union-NextGenerationEU program. This work used the Beronia cluster (Universidad de La Rioja), which is supported by FEDER-MINECO grant number UNLR-094E-2C-225. The authors also acknowledge CSC-IT Center for Science, Finland and the Finnish Grid and Cloud Infrastructure (persistent